Reinforced Concrete Membrane Element Formulations

By F. J. Vecchio[1]

Abstract: Finite-element formulations are presented for the analysis of reinforced concrete membrane structures. Cracked reinforced concrete is treated as an orthotropic material based on a smeared, rotating crack model. Secant-stiffness moduli are defined for concrete and reinforcement, and these are used in the development of linear displacement rectangular and triangular membrane finite elements. Procedures are discussed by which these elements can then be incorporated into a nonlinear analysis algorithm. Extensions to the formulations are also described that permit the consideration of prestrain effects in the component materials such as prestressing of the reinforcement, shrinkage of the concrete, or thermal expansion. The constitutive relations currently utilized are those of the modified compression field theory, although the element formulations are sufficiently generic to easily accommodate other constitutive models. A numerical example is provided to illustrate the simplicity of the calculation procedure and the good convergence characteristics and numerical stability of the formulations. Corroboration with experimental data is also discussed. Finally, the capabilities and application potential of the analysis procedure are demonstrated in sample analyses.

Introduction

Procedures for nonlinear finite element analysis of reinforced concrete structures have reached a stage in development and acceptance where they are regularly used in design/analysis applications (e.g., see Fig. 1). Various development approaches have been taken (e.g., Balakrishnam and Murray 1988; Niwa et al. 1981; Barzegar-Jamshidi and Schnobrich 1986; Stevens et al. 1987), differing in such aspects as stiffness formulation (tangent stiffness versus secant stiffness), constitutive modeling and element preference. Regardless of the approach taken, however, it appears that the usefulness of any particular procedure depends on two key factors. First, the formulation must incorporate a set of constitutive relations for concrete and reinforcement that realistically model cracked reinforced concrete behavior. Second, the formulation must be numerically compliant and stable over a wide range of structural design and loading conditions.

An alternative procedure was recently developed whereby linear elastic finite element routines could be easily modified to enable nonlinear analysis of reinforced concrete membrane structures. The procedure is based on an iterative, secant stiffness formulation, and employs constitutive relations for concrete and reinforcement based on the modified compression field theory (Vecchio and Collins 1986). Predictions from the proposed formulation were compared against experimental results, and excellent accuracy was found in both strength and deformation response. Details of the procedure formulation, and experimental verification, are documented in a previous paper (Vecchio 1989).

In this paper, further elaboration is given to the secant stiffness formulations central to the proposed method. Specifically, element stiffness matrix

[1]Assoc. Prof., Dept. of Civ. Engrg., Univ. of Toronto, Toronto, Ontario, Canada M5S 1A4.

Note. Discussion open until August 1, 1990. To extend the closing date one month, a written request must be filed with the ASCE Manager of Journals. The manuscript for this paper was submitted for review and possible publication on February 5, 1988. This paper is part of the ***Journal of Structural Engineering***, Vol. 116, No. 3, March, 1990. ©ASCE, ISSN 0733-9445/90/0003-0730/$1.00 + $.15 per page. Paper No. 24443.

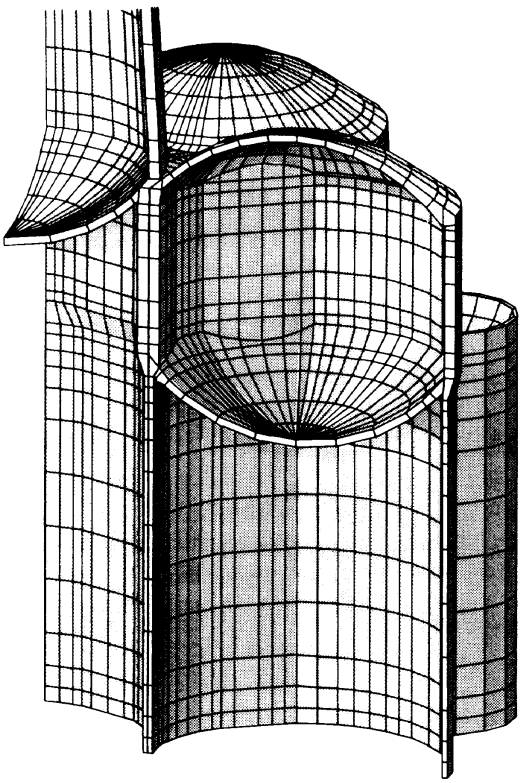

FIG. 1. Finite Element Model of Offshore Structure

formulations are derived for rectangular and triangular linear displacement elements. A solution algorithm is described, and modifications are introduced which enable material prestrains (e.g., reinforcement prestressing, concrete shrinkage) to be taken into account. The computational simplicity, numerical stability, and application potential of the formulation are demonstrated through sample analyses.

Material Stiffness Formulations

In constructing the stiffness matrix $[k]$ for an individual element, a material stiffness matrix $[D]$ is required to relate stresses $\{f\}$ to strains $\{\epsilon\}$, i.e.

$$\{f\} = [D]\{\epsilon\} \quad \ldots\ldots (1)$$

where $\{f\} = [f_x \; f_y \; v_{xy}]$ and $\{\epsilon\} = [\epsilon_x \; \epsilon_y \; \gamma_{xy}]$. For a linear elastic isotropic material, in a plane stress state,

$$[D] = \frac{E}{(1-\nu^2)} \begin{bmatrix} 1 & \nu & 0 \\ \nu & 1 & 0 \\ 0 & 0 & (1-\nu)/2 \end{bmatrix} \quad \ldots\ldots (2)$$

To reflect the nonlinear behavior of reinforced concrete, $[D]$ is modified according to an appropriate set of constitutive laws. Its form also depends on the type of stiffness moduli used. The formulations that follow assume a secant stiffness approach.

Assume a global reference system X, Y and an element reference system x, y as defined in Fig. 2. Further, assume the n reinforcement orientations within the element are measured in x_i', y_i' axes systems ($i = 1, \ldots, n$). The angles β, ϕ, and α_i are used to relate directions.

The material stiffness matrix $[D]$ for the element is to be defined with

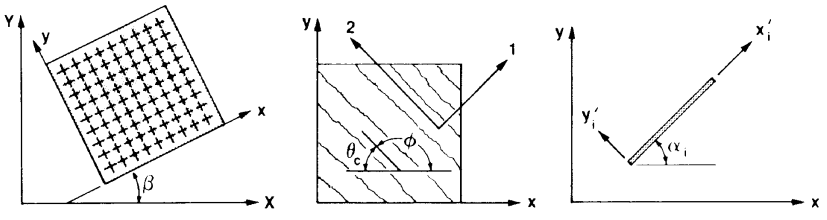

(a) Element in Global System (b) Concrete Component (c) Reinforcement Components

FIG. 2. Reference Systems for Reinforced Concrete Element

respect to the global X, Y axes. This is done by first defining a stiffness matrix for the concrete component, $[D_c]'$, and for each of the reinforcement components, $[D_s]_i'$. The total stiffness is then determined by combining the contributions from each of the components, using appropriate transformations to take into account the anisotropy of the materials.

Cracked reinforced concrete can be treated as an orthotropic material with its principal axes 1,2 corresponding to the direction of the principal average tensile strain and principal average compressive strain (i.e., crack direction), respectively (see Fig. 2). Further, after cracking, Poisson's effect can be considered negligible. Thus, the concrete material stiffness matrix $[D_c]'$, evaluated with respect to the principal 1,2 axes system, is

$$[D_c]' = \begin{bmatrix} \bar{E}_{c2} & 0 & 0 \\ 0 & \bar{E}_{c1} & 0 \\ 0 & 0 & \bar{G}_c \end{bmatrix} \quad \ldots\ldots (3)$$

where $\bar{E}_{c1}$, $\bar{E}_{c2}$, and $\bar{G}_c$ are secant moduli. At a particular stress/strain state, the secant moduli are evaluated as follows:

$$\bar{E}_{c1} = \frac{f_{c1}}{\epsilon_{c1}} \quad \ldots\ldots (4)$$

$$\bar{E}_{c2} = \frac{f_{c2}}{\epsilon_{c2}} \quad \ldots\ldots (5)$$

and

$$\bar{G}_c = \frac{\bar{E}_{c1} \cdot \bar{E}_{c2}}{\bar{E}_{c1} + \bar{E}_{c2}} \quad \ldots\ldots (6)$$

where ϵ_{c1} = concrete average principal tensile strain; ϵ_{c2} = concrete average principal compressive strain; f_{c1} = concrete average tensile stress in the 1-direction; and f_{c2} = concrete average compressive stress in the 2-direction.

For each reinforcement component, a corresponding matrix $[D_s]_i'$ is evaluated as

$$[D_s]_i' = \begin{bmatrix} \rho_i \bar{E}_{si} & 0 & 0 \\ 0 & 0 & 0 \\ 0 & 0 & 0 \end{bmatrix} \quad \ldots\ldots (7)$$

where ρ_i = reinforcement ratio; and $\bar{E}_{si}$ = secant modulus. Again, the modulus is determined for a particular stress/strain state using the relationship

$$\bar{E}_{si} = \frac{f_{si}}{\epsilon_{si}} \quad \ldots\ldots (8)$$

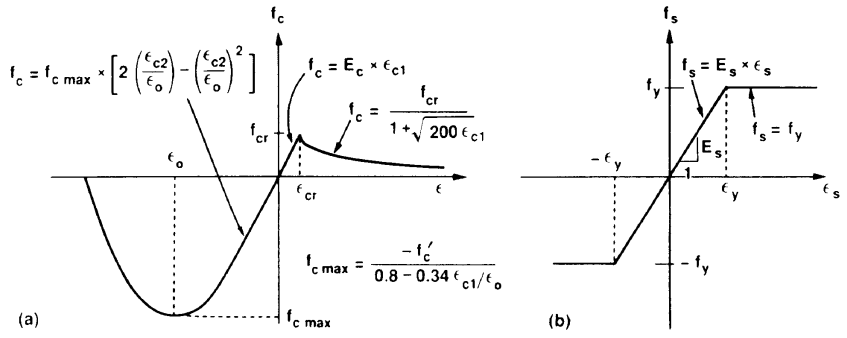

FIG. 3. Constitutive Relations for Concrete and Reinforcement: (*a*) Concrete; (*b*) Reinforcement

where ϵ_{si} = average strain in the reinforcement; and f_{si} = average stress.

Transformations must be applied to convert the component stiffnesses to the global system. Thus, the total material stiffness matrix $[D]$ is evaluated as

$$[D] = [D_c] + \sum_{i=1}^{n} [D_s]_i \quad \ldots\ldots (9)$$

where

$$[D_c] = [T_c]^T [D_c]' [T_c] \quad \ldots\ldots (10)$$

and

$$[D_s]_i = [T_s]_i^T [D_s]_i' [T_s]_i \quad \ldots\ldots (11)$$

The transformation matrix $[T]$ is given by

$$[T] = \begin{bmatrix} \cos^2\psi & \sin^2\psi & \cos\psi \sin\psi \\ \sin^2\psi & \cos^2\psi & -\cos\psi \sin\psi \\ -2\cos\psi \sin\psi & 2\cos\psi \sin\psi & (\cos^2\psi - \sin^2\psi) \end{bmatrix} \quad \ldots\ldots (12)$$

where, for the concrete component,

$$\psi = \phi + \beta = 180° + \beta - \theta_c \quad \ldots\ldots (13)$$

and for the reinforcement components

$$\psi = \alpha_i + \beta \quad \ldots\ldots (14)$$

Note that $[T]$ differs for each of the components. The resulting matrix $[D]$ is a full, symmetric matrix, dependent on the orientation of the element in the global space.

To model nonlinear material response, the constitutive relations contained in the modified compression field theory (MCFT) (Vecchio and Collins 1986) (see Fig. 3) have been adopted. Thus, for concrete in compression, the relations used to model strain softening effects are

$$f_{c2} = f_{c2\max} \left[2\left(\frac{\epsilon_{c2}}{\epsilon_0}\right) - \left(\frac{\epsilon_{c2}}{\epsilon_0}\right)^2 \right] \quad \ldots\ldots (15)$$

where

$$f_{c2\max} = \frac{-f_c'}{0.8 - \dfrac{0.34\epsilon_{c1}}{\epsilon_0}} \geq -f_c' \quad \ldots\ldots (16)$$

For concrete in tension, prior to cracking, a linear relation is used, i.e.,

$$f_{c1} = E_c \cdot \epsilon_{c1}, \qquad 0 \leq \epsilon_{c1} \leq \epsilon_{cr} \quad \ldots\ldots (17)$$

where

$$E_c = \frac{2f'_c}{\epsilon_0} \quad \ldots\ldots (18)$$

$$\epsilon_{cr} = \frac{f_{cr}}{E_c} \quad \ldots\ldots (19)$$

$$f_{cr} = 0.33\sqrt{f'_c}\ (\text{MPa}) \quad \ldots\ldots (20)$$

After cracking, concrete in tension is made to reflect tension stiffening effects through the following relation

$$f_{c1} = \frac{f_{cr}}{1 + \sqrt{200 \cdot \epsilon_{c1}}} \quad \ldots\ldots (21)$$

The MCFT assumes a bilinear stress-strain relation for reinforcement, i.e.,

$$f_{si} = E_s \cdot \epsilon_{si} \leq f_{yi} \quad \ldots\ldots (22)$$

However, Eq. 22 can be modified to reflect strain hardening effects, or curvilinear response more appropriate for prestressing reinforcement.

Note while the MCFT relations have been used in the analyses to follow, the stiffness formulations are such that any realistic set of stress-strain relations can be easily implemented.

Element Stiffness Formulations

Having determined an appropriate material stiffness $[D]$, the stiffness matrix $[k]$ for a particular element can be evaluated using standard procedures (e.g., Yang 1986). The computations involved can be summarized as

$$[k] = \int [B]^T [D][B] dV \quad \ldots\ldots (23)$$

where the shape matrix $[B]$ is dependent on the assumed element displacement functions.

Formulations were derived in closed-form for the rectangular and the triangular linear displacement elements shown in Fig. 4. The corresponding element stiffness matrix coefficients are given in Appendix I. It should be noted that, because of the full nature of the material stiffness matrix $[D]$, the coefficients derived differ from those commonly reported for similar iso-

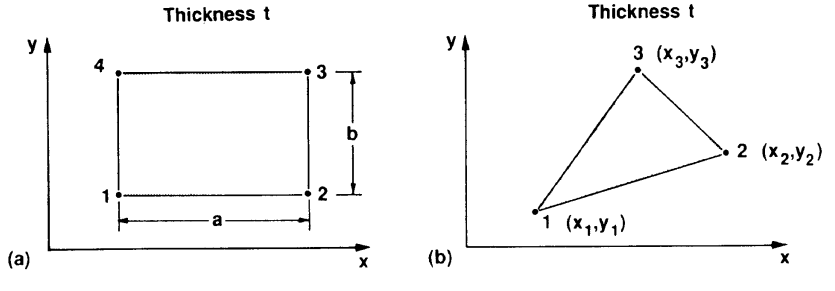

FIG. 4. Geometry of Linear Displacement Elements: (*a*) Rectangular Element; (*b*) Triangular Element

tropic elements. Note too that the element stiffness matrices [k] remain symmetrical.

The procedure outlined above can be applied in formulating higher order elements, although resort to numerical integration techniques may be required.

Accounting for Prestrains

The secant stiffness approach to element formulation readily permits the inclusion of prestrain effects in the component materials of an element. This enables analyses to account for prestressing in the reinforcement, shrinkage or expansion of the concrete, thermal expansion of either the concrete or reinforcement, or other types of strain offset effects.

Consider for example a uniaxial reinforced concrete element as shown in Fig. 5. The element may be subjected to a concrete shrinkage [e.g., Fig. 5(*a*)], prestressing in the reinforcement [e.g., Fig. 5(*b*)], or any combination of prestrains in the component materials. In any case, the initial free prestrains in the concrete, ϵ_c^o, and in the reinforcement, ϵ_s^o, are known. Under an externally applied load F, the element exhibits a total measurable strain ϵ.

In determining secant stiffness moduli for the component materials of the element, the strain values to be used in Eqs. 4, 5, and 8 are the strains due to stress (see Fig. 5). Thus, for the concrete

$$\epsilon_c = \epsilon - \epsilon_c^o \quad \ldots\ldots (24)$$

and for the reinforcement

$$\epsilon_s = \epsilon - \epsilon_s^o \quad \ldots\ldots (25)$$

The prestrains are evaluated as

$$\epsilon_c^o = \alpha_c \cdot \Delta T - \epsilon_{sh} + \epsilon_{ce} \quad \ldots\ldots (26)$$

and

$$\epsilon_s^o = \alpha_s \cdot \Delta T - \Delta\epsilon_p + \epsilon_{se} \quad \ldots\ldots (27)$$

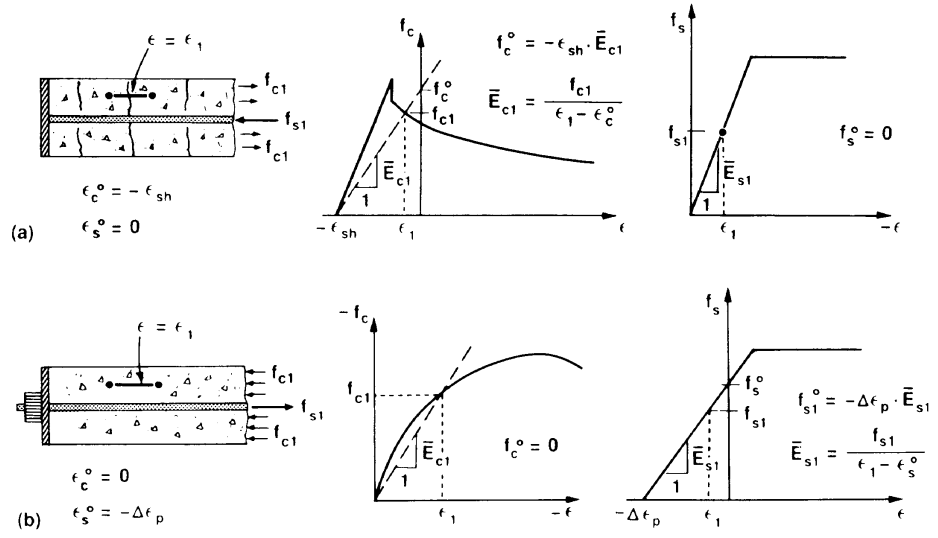

FIG. 5. Secant Moduli for Element with Prestrains: (*a*) with Concrete Shrinkage Prestrain; (*b*) with Prestressed Reinforcement

where α_c = coefficient of thermal expansion of the concrete; ΔT = change in temperature; ϵ_{sh} = concrete shrinkage strain; ϵ_{ce} = concrete expansion strain accounting for alkali reactivity or any other volume prestrain effect; α_s = coefficient of thermal expansion of reinforcement steel; $\Delta\epsilon_p$ = prestressing strain; and ϵ_{se} accounts for any other prestrain effect in the reinforcement. Offset strains arising from previous loading conditions (e.g., strain offset in the reinforcement due to prior yielding), from cyclic loading effects, or from creep could be accounted for in a similar manner.

A prestrain pseudo-force F^* can be defined as

$$F^* = A \cdot (f_c^o + \rho_{s1} \cdot f_s^o) = A \cdot (\bar{E}_{c1} \cdot \epsilon_c^o + \rho_{s1} \cdot \bar{E}_{s1} \cdot \epsilon_s^o) \quad (28)$$

Thus, the total force considered to be acting on the element is

$$F' = F + F^* \quad (29)$$

where F = externally applied load. The axial stiffness of the element k is

$$k = [\bar{E}_{c1} + \rho_{s1} \cdot \bar{E}_{s1}] \cdot \frac{A}{L} \quad (30)$$

where A = element cross-sectional area; and L = length. The elongation of the member is

$$\Delta L = \frac{F'}{k} \quad (31)$$

and thus the strain is determined as

$$\epsilon = \frac{\Delta L}{L} = \frac{F'}{kL} = \frac{F + A \cdot (\bar{E}_{c1} \cdot \epsilon_c^o + \rho_{s1} \cdot \bar{E}_{s1} \cdot \epsilon_s^o)}{A \cdot (\bar{E}_{c1} + \rho_{s1} \cdot \bar{E}_{s1})} \quad (32)$$

Note, however, that the total strain (ϵ) and the secant moduli ($\bar{E}_{c1}, \bar{E}_{s1}$) are interdependent and so an iterative solution is required.

This pseudo-force approach to accounting for prestrains can be generalized for two-dimensional membrane elements. Prestrains must be defined for the concrete and each of the reinforcement components of an element, thus

$$[\epsilon_c^o] = \begin{bmatrix} \epsilon_{cx}^o \\ \epsilon_{cy}^o \\ \epsilon_{cxy}^o \end{bmatrix} = \begin{bmatrix} \epsilon_c^o \\ \epsilon_c^o \\ 0 \end{bmatrix} \quad (33)$$

and

$$[\epsilon_s^o]_i = \begin{bmatrix} \epsilon_{sxi}^o \\ \epsilon_{syi}^o \\ \epsilon_{sxyi}^o \end{bmatrix} = \begin{bmatrix} \epsilon_{si}^o \cdot (1 + \cos 2\alpha_i)/2 \\ \epsilon_{si}^o \cdot (1 - \cos 2\alpha_i)/2 \\ \epsilon_{si}^o \cdot \sin 2\alpha_i \end{bmatrix} \quad (34)$$

From the prestrains, free joint displacements are determined as functions of the element geometry, i.e.,

$$[r_c^o] = \int [\epsilon_c^o] dA \quad (35)$$

$$[r_s^o] = \int [\epsilon_s^o] dA \quad (36)$$

Given the free displacements, the prestrain joint forces can be evaluated as

$$[F^*] = [k_c][r_c^o] + \sum_{i=1}^{n} [k_s]_i [r_s^o]_i \quad (37)$$

where $[k_c]$ and $[k_s]_i$ are the element stiffness matrices evaluated separately

for each of the components using the formulations described previously. The prestrain forces are added to the externally applied joint loads to determine the total force vector $[F']$. A routine solution procedure is used thereafter to determine joint displacements, and hence final element strains. Having calculated the element strains $[\epsilon]$, the element stresses can be found from

$$[f] = [D_c]([\epsilon] - [\epsilon_c^o]) + \sum_{i=1}^{n} [D_s]_i([\epsilon] - [\epsilon_s^o]_i) \quad \ldots\ldots\ldots\ldots\ldots\ldots\ldots\ldots \quad (38)$$

IMPLEMENTATION

Nonlinear analyses of reinforced concrete membranes can be achieved by incorporating the element formulations described above into an iterative linear elastic analysis procedure. Through each iteration, the material stiffness $[D]$ and element stiffness $[k]$ matrices are progressively refined until convergence is achieved. A flow chart summarizing the solution procedure is given in Fig. 6.

In regards to the computation algorithm, the following should be noted.

1. As the stiffness matrices change through each iteration, so too will the prestrain force vector $[F^*]$. Hence, the total force vector $[F']$ must be recalculated through each iteration (Step 9).
2. If no element prestrains are present, then the component stiffness matrices

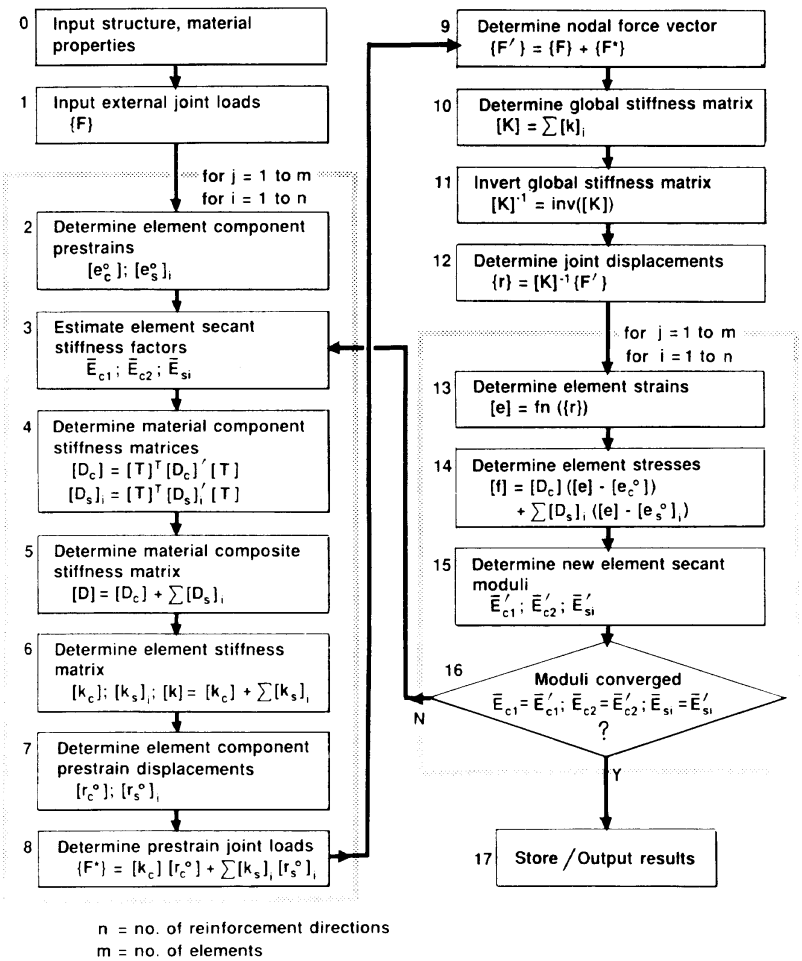

FIG. 6. Solution Procedure for Nonlinear Analysis

$[k_c]$ and $[k_s]_i$ need not be evaluated individually; the total stiffness $[k]$ can be determined directly from the composite material stiffness $[D]$. If prestrains are present, $[k] = [k_c] + \Sigma[k_s]_i$ where the component stiffnesses $[k_c]$ and $[k_s]_i$ are determined from the stiffness formulations (Appendix I) using the material stiffnesses $[D_c]$ and $[D_s]_i$, respectively.

3. Given element strains as determined in Step 13, the strains and stresses in the component materials are determined from compatibility and stress-strain relations. These are then used to determine new values for the secant stiffness moduli (Step 16) using the formulations previously discussed. If the newly computed moduli are not equal to those assumed in Step 3, a further iteration of the solution is required. The newly computed moduli can be used to propagate the solution.

SAMPLE CALCULATIONS

Consider panel specimen PB21, shown in Fig. 7(*a*), tested by Bhide and Collins (1987). The materials properties of the element are given as

$f'_c = 21.8$ MPa $\quad f_{cr} = 1.54$ MPa $\quad \epsilon_0 = -0.0018$

$E_c = 24{,}200$ MPa $\quad \nu = 0.30 \quad E_s = 200{,}000$ MPa

$\rho_x = 0.02195 \quad \rho_y = 0 \quad f_{yx} = 402$ MPa

An analysis is to be conducted for the uniform stress condition

$f_x = 3.10$ MPa $\quad f_y = 0 \quad v_{xy} = 1.0$ MPa

The finite element model used, comprised of a single rectangular element, is shown in Fig. 7(*b*). (Note that this specimen, reinforced in one direction only, represents a difficult problem from a computational viewpoint. Ignoring tension stiffening effects, as most formulations do, will result in an inability of the panel to sustain loads beyond cracking.)

In implementing the solution procedure summarized in Fig. 6, the strains corresponding to the given loads are found to be

$$[\epsilon] = [0.706 \quad 0.707 \quad 1.507] \times 10^{-3}$$

Some pertinent values computed during the various iterations of the solution process are charted in Table 1. A detailed set of calculations corresponding to the 11th iteration is given in Appendix II. Note that the first cycle began with the assumption of linear isotropic behavior (i.e., as in Eq. 2) in defining

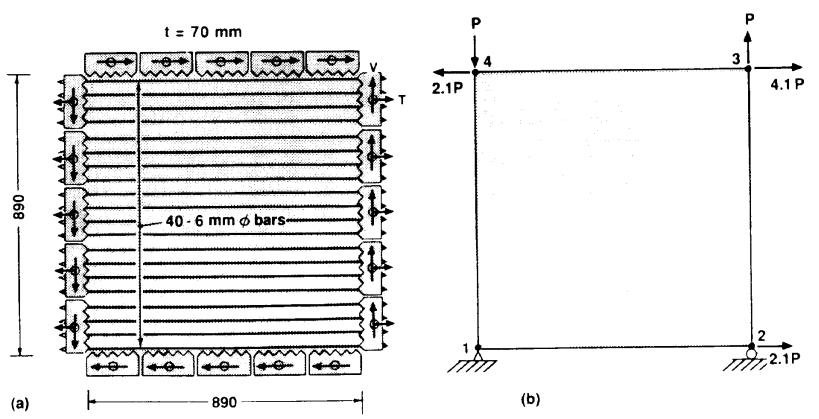

FIG. 7. Panel Specimen PB21: (*a*) Specimen Properties; (*b*) Finite Element Model

TABLE 1. Summary of Analysis of Panel PB21

Iteration number (1)	Secant Moduli			Stiffness Coefficients						Displacements				Strains			
	$\bar{E}_{c1}$ (MPa) (2)	$\bar{E}_{c2}$ (MPa) (3)	$\bar{G}_c$ (MPa) (4)	D_{11} (MPa) (5)	D_{12} (MPa) (6)	D_{13} (MPa) (7)	D_{22} (MPa) (8)	D_{23} (MPa) (9)	D_{33} (MPa) (10)	u_2 (mm) (11)	u_3 (mm) (12)	u_4 (mm) (13)	v_3, v_4 (mm) (14)	ϵ_x (10^{-3}) (15)	ϵ_y (10^{-3}) (16)	γ_{xy} (10^{-3}) (17)	θ (degrees) (18)
1	24,200	24,200	9,310	26,593	7,978	0	26,593	0	9,310	0.114	0.210	0.096	−0.034	0.128	−0.038	0.107	73.6
2	9,148	23,629	6,595	14,237	478	−1,233	22,008	−2,688	7,067	0.208	0.376	0.168	0.016	0.234	0.018	0.189	69.5
3	4,645	23,612	3,881	10,010	1,384	−1,549	19,874	−4,704	5,268	0.316	0.623	0.307	0.051	0.355	0.057	0.345	65.4
4	2,739	23,287	2,451	8,366	2,321	−1,880	17,411	−5,892	4,773	0.408	0.889	0.481	0.108	0.458	0.122	0.540	60.9
5	1,877	22,936	1,735	8,011	3,219	−2,463	14,756	−6,473	4,955	0.472	1.127	0.656	0.185	0.530	0.207	0.736	56.8
6	1,435	22,612	1,349	8,253	3,911	−3,135	12,363	−6,563	5,261	0.515	1.323	0.808	0.266	0.579	0.299	0.908	53.6
7	1,180	22,336	1,121	8,685	4,344	−3,713	10,534	−6,394	5,466	0.546	1.479	0.933	0.341	0.613	0.383	1.048	51.2
8	1,022	22,105	978	9,111	4,584	−4,142	9,241	−6,154	5,561	0.568	1.599	1.032	0.405	0.638	0.455	1.159	49.5
9	921	21,917	883	9,464	4,709	−4,442	8,346	−5,928	5,592	0.584	1.692	1.108	0.457	0.656	0.514	1.245	48.3
10	852	21,767	820	9,740	4,773	−4,650	7,724	−5,740	5,592	0.596	1.762	1.166	0.499	0.669	0.560	1.310	47.4
11	805	21,649	776	9,948	4,805	−4,794	7,287	−5,593	5,580	0.604	1.815	1.211	0.531	0.679	0.596	1.360	46.7
12	771	21,558	745	10,104	4,820	−4,894	6,976	−5,481	5,565	0.611	1.855	1.244	0.555	0.686	0.624	1.398	46.3
13	748	21,489	723	10,220	4,827	−4,965	6,754	−5,396	5,550	0.615	1.884	1.269	0.574	0.691	0.645	1.426	45.9
14	731	21,438	707	10,305	4,830	−5,016	6,593	−5,332	5,537	0.619	1.906	1.288	0.588	0.695	0.661	1.447	45.7
15	719	21,399	695	10,369	4,831	−5,052	6,476	−5,285	5,527	0.621	1.923	1.302	0.599	0.698	0.672	1.462	45.5
20	692	21,310	670	10,509	4,830	−5,130	6,223	−5,177	5,500	0.627	1.959	1.333	0.622	0.704	0.699	1.497	45.1
21	690	21,303	668	10,519	4,830	−5,136	6,205	−5,171	5,498	0.628	1.962	1.335	0.624	0.705	0.701	1.500	45.1
25	686	21,290	665	10,540	4,829	−5,147	6,168	−5,155	5,494	0.628	1.968	1.339	0.627	0.706	0.705	1.505	45.0
30	685	21,285	664	10,547	4,829	−5,150	6,156	−5,150	5,493	0.629	1.970	1.341	0.629	0.706	0.706	1.507	45.0
35	685	21,284	664	10,548	4,829	−5,151	6,153	−5,149	5,492	0.629	1.970	1.341	0.629	0.706	0.707	1.507	45.0

Note: $\bar{E}_{s1}$ = 200,000 MPa for all iterations.

the [D] matrix. Each successive iteration was based on the strains calculated in the previous cycle.

Convergence Characteristics

The method, as currently formulated, utilizes the strains determined from the previous iteration to redefine element stiffnesses and, hence, propagate the analysis. Typically, 20 to 30 iterations are required to converge to a final solution. This number has been found to be relatively insensitive to structure size (i.e., number of elements) or element properties (e.g., reinforcement patterns), provided that the structure's ultimate load capacity has not been exceeded. (Localized post-ultimate behavior is accounted for without difficulty). In numerous analyses conducted to-date, the numerical stability of the procedure has been remarkably good.

Shown in Fig. 8 are the convergence patterns exhibited by the [D]-matrix coefficients and the element strains in the sample solution described above. The stiffness coefficients initially undergo marked variation as behavior changes from uncracked isotropic to cracked orthotropic response. Thereafter, the stiffness coefficients rapidly converge to stable values. The strain quantities also rapidly converge, generally in a monotonic manner. Note that convergence to within 1% of final values, for this relatively difficult case (i.e., panel reinforced in one direction only), is obtained after about 20 iterations.

Convergence is equally good if the initial (or intermediate) strain values are greater than the final results. However, in the sample problem, where the structure consists of one element only, convergence will not be assured if the initial strains represent a post-ultimate condition. In the more general case of multi-element structures, local post-ultimate strain conditions will cause a relieving of load to neighboring elements. This will act to reduce

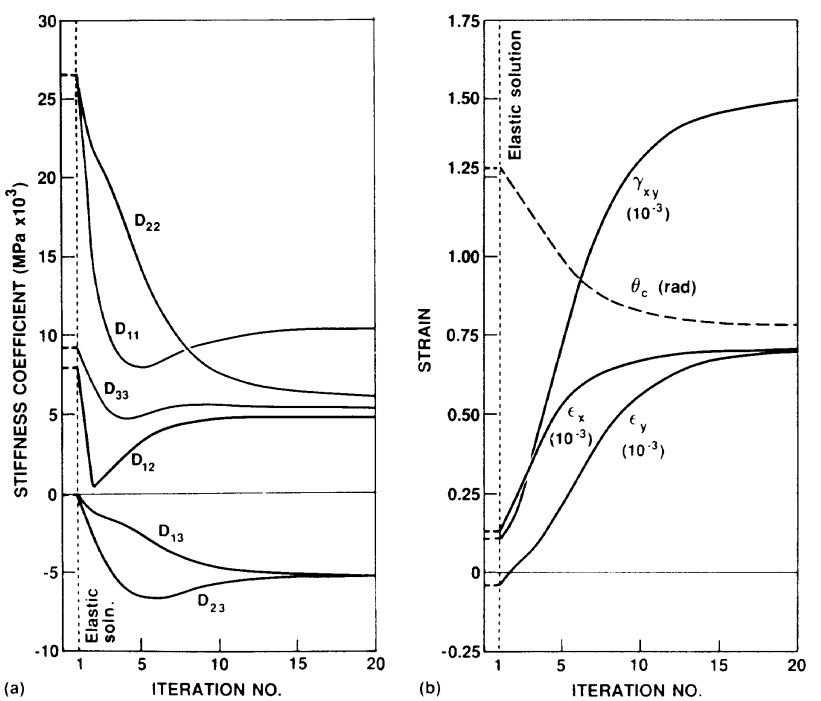

FIG. 8. Convergence Characteristics of PB21 Analysis: (*a*) Stiffness Coefficients; (*b*) Strains

the local strains, thus increasing stiffness and restoring equilibrium. Numerical stability under these conditions has also been found to be very good.

EXPERIMENTAL CORROBORATION

The formulations described can represent completely any constitutive model which relates principal stresses to principal strains in the concrete, and axial stresses to axial strains in the reinforcement. Inaccuracies which may arise, apart from improper mesh size in consideration of the simplicity of the elements, will relate entirely to the appropriateness of the constitutive models used.

The stress-strain formulations currently employed are those of the MCFT. They were derived from an extensive series of panel tests (Vecchio and Collins 1986) and appear to capture in a simple way the nonlinear behavior of concrete. In predicting the results of 19 panels involving primarily concrete shear/crushing failures, under a variety of reinforcement and loading conditions, the ratio of experimental to theoretical ultimate load had a mean value of 1.002 and a coefficient of variation of 10.0%. Deformation responses were predicted equally well. Other researchers (e.g., Ang 1985; Mau and Hsu 1987) report similar success in the use of these relations.

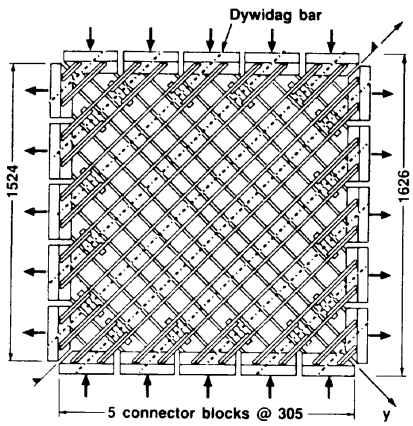

Specimen	f'_c (MPa)	ϵ_0 ($\times 10^{-3}$)	ρ_x (%)	ρ_y (%)	ρ_{px} (%)	f_{px} (MPa)
PP1	27.0	2.17	1.95	0.65	0.00	0.0
PP2	28.1	2.38	1.30	0.65	0.29	2.08
PP3	27.7	1.92	0.65	0.65	0.59	4.39

f_y = 480 MPa for conventional reinforcement (ρ_x, ρ_y)
f_y = 910 MPa for prestressing reinforcement (ρ_{px})

(a) Specimen Details

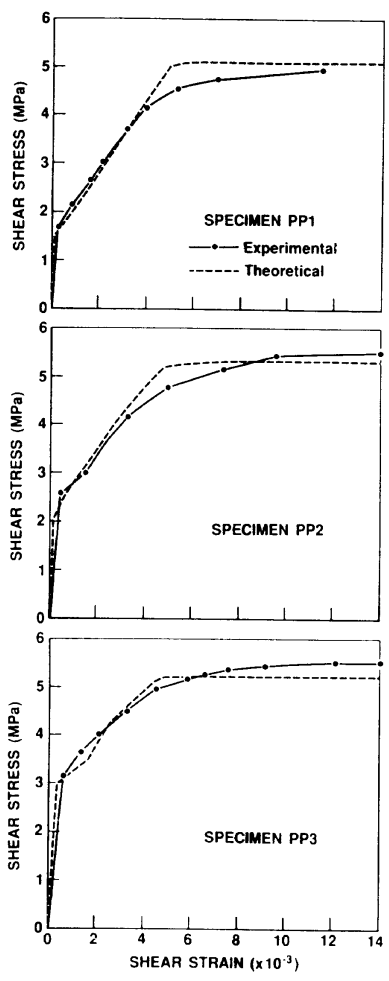

(b) Predicted vs. Observed Response

FIG. 9. Partially Prestressed Panels Tested by Marti and Meyboom (1987)

Experimental corroboration with reinforced concrete specimens not involving prestrain effects is discussed elsewhere (Vecchio 1989). Experimental data relating to membrane specimens with prestrains could not be found in the literature. However, Marti and Meyboom (1987) describe a preliminary investigation in which panel specimens with partial prestressing were tested. The panels were subjected to pure membrane shear relative to the orthogonal reinforcement, with specimen properties and loading details as shown in Fig. 9(*a*). The observed response of each panel, together with the theoretical behavior based on a one-element analysis, is given in Fig. 9(*b*). It can be seen that both the ultimate strength and the deformation of the panels were accurately predicted.

Sample Analyses

The capabilities and limitations of the procedure presented are reflected in the two sample analyses discussed below.

Consider Panel W2 tested by Cervenka (1970), which has long served as a benchmark test for calibrating finite element formulations. The 760 mm deep, 75 mm thick panel is simply supported over a 1,720 mm span, and is subjected to a concentrated load at the midspan. Horizontal reinforcement in the lower 150 mm region is at 1.83%; above, the horizontal reinforcement ratio is at 0.92%. Vertical reinforcement is provided at 0.92%. Other pertinent details and material properties are given in Fig. 10(*a*). An analysis

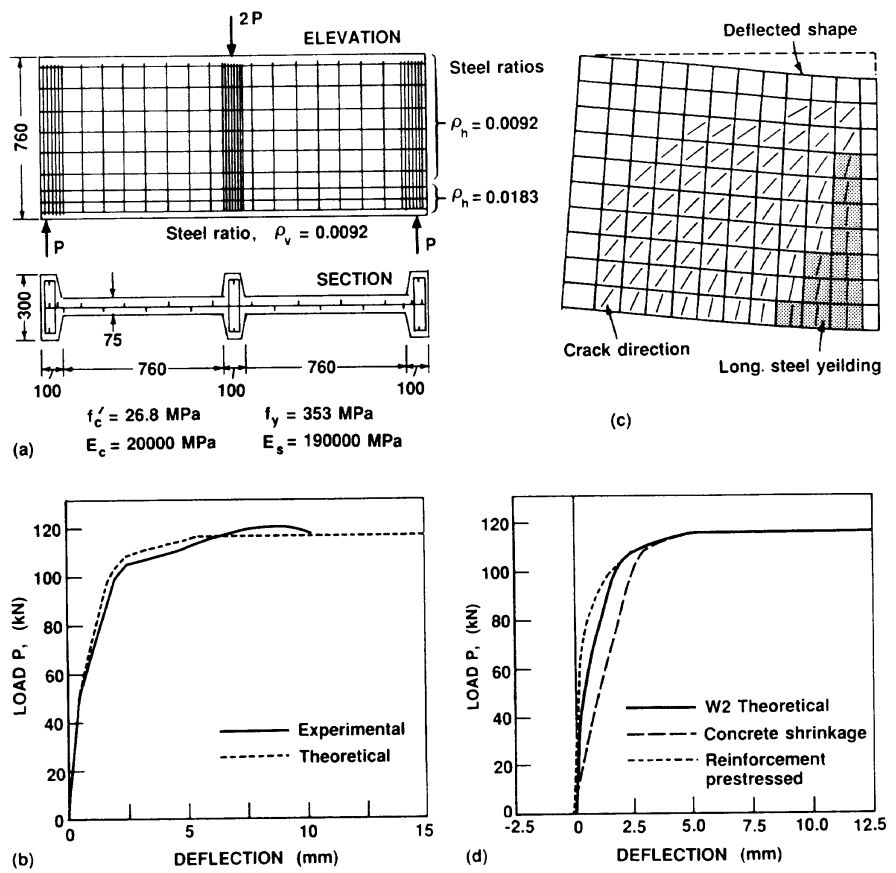

FIG. 10. Analysis of Cervenka Panel W2: (*a*) Specimen Details; (*b*) Load-Deflection Response; (*c*) Conditions at P = 110 kN; and (*d*) Response under Hypothetical Conditions

was conducted to determine the theoretical load-deformation response of the panel. The computed response is compared to the observed response in Fig. 10(*b*), based on an analysis using the element mesh shown in Fig. 10(*c*). The correlation is generally very good, with pre-cracking stiffness, post-cracking stiffness, post-yield stiffness, and ultimate load capacity well-predicted. The experimental response exhibited a slightly higher ultimate capacity, with a distinct peak and drop-off, likely as a result of strain hardening effects in the reinforcement. Strain hardening was not considered in the theoretical analysis, although the ability to do so exists. Also, it is seen that the theoretical analysis slightly underpredicts post-cracking deformations. This may be a result of the tension stiffening model (i.e., Eq. 21) being too stiff, or due to shrinkage stresses affecting the observed response. Predicted deflections, cracking patterns, and reinforcement yielding at a load level near failure are shown in Fig. 10(*c*).

Two additional analyses were conducted on Panel W2, assuming hypothetical conditions. In the first, the concrete in the 75 mm-thick regions of the panel was assumed to have undergone a shrinkage strain of 0.4×10^{-3}; concrete in the thicker regions was given no shrinkage strain. This resulted in the panel being precracked to some extent. The second hypothetical condition had the horizontal reinforcement in the bottom regions of the panel (i.e., where $\rho = 0.0183$) prestressed with a strain $\Delta\epsilon_p = 1.5 \times 10^{-3}$, but with the yield strength unaltered. The load-deflection response for each con-

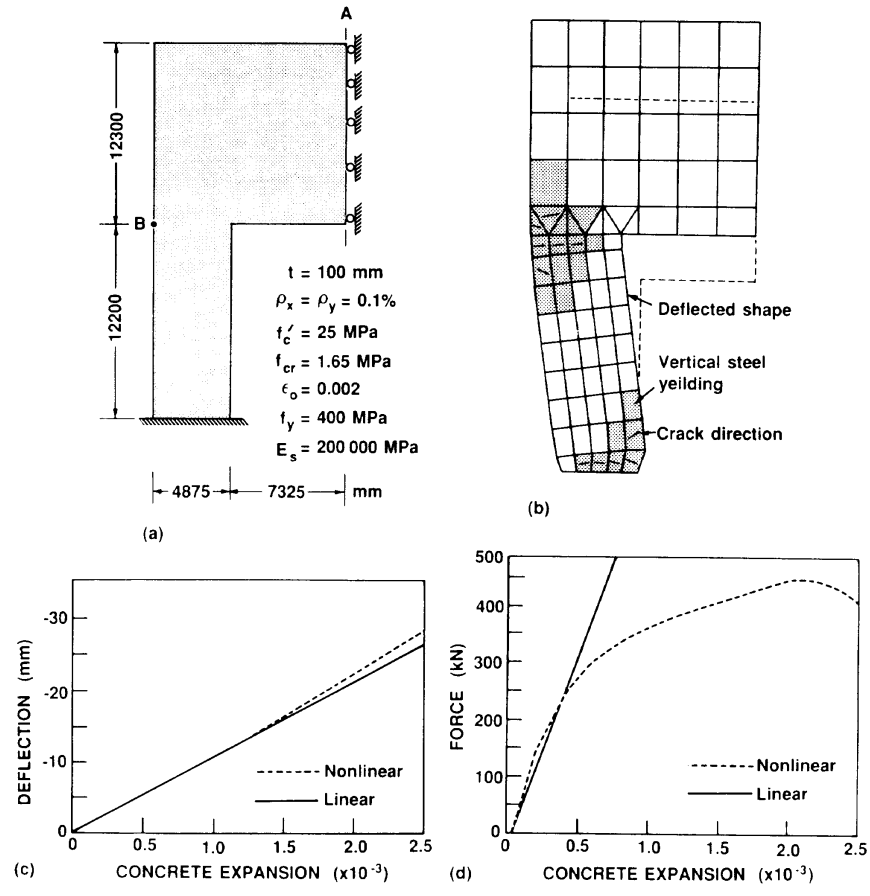

FIG. 11. Analysis of Dam Section Subjected to Concrete Expansion: (*a*) Structure Details; (*b*) Conditions at $\epsilon_{cs} = 2.0 \times 10^{-3}$; (*c*) Horizontal Deflection at Point B; and (*d*) Thrust at Section A

dition was computed and is shown in Fig. 10(*d*). As expected, concrete shrinkage resulted in a significant decrease in the stiffness of the panel, whereas prestressing increased the initial stiffness. Prestressing also imparted a small initial upward deflection on the panel; shrinkage caused no initial deflection. Neither condition affected the ultimate load capacity of the panel. At intermediate load levels, however, deflections differ in excess of 200%.

An analysis was also conducted of a dam structure in which observed damage was postulated to be the result of concrete expansion due to alkali reactivity. A portion of the structure, representing a 100 mm slice through a penstock section, is shown in Fig. 11(*a*). Nominal reinforcement of 0.1% is provided in both the horizontal and vertical directions. Analyses were conducted for concrete expansion strains ranging up to 2.5×10^{-3}. The deformation and cracking patterns in the structure corresponding to an expansion of 2.0×10^{-3} are shown in Fig. 11(*b*). Note that the structure is experiencing a flexural failure, rather than one involving brittle shear as had been anticipated. The horizontal deflection of the structure, and the compressive thrust developed at the rightmost section, are compared to values computed from linearly elastic analyses in Fig. 11(*c*) and (*d*). The deflections are seen to follow essentially a linear progression. The forces developed, however, show exceeding nonlinear behavior and are considerably less than those computed from a linear analysis. A gradual softening of the force response is seen as cracking propagates at the top and bottom interfaces. As the expansion strain exceeds 2.2×10^{-3}, yielding of the vertical reinforcement results in a downturn in thrust.

Conclusions

Cracked reinforced concrete can effectively be treated as an orthotropic material, with secant stiffness moduli defined for the directions parallel and perpendicular to the crack direction. The material, as such, is characterized by a full, symmetric stiffness matrix [*D*], combining the contributions from concrete and reinforcement. The stiffness coefficients can be calculated according to any realistic constitutive model. Finite elements can thus be formulated, incorporating advanced material behavior models, by using standard procedures. This leads to a simple, but effective, means of performing nonlinear analyses of concrete membranes.

The secant stiffness formulations presented are simple and generic in concept. Finite elements formulated accordingly retain a general form that permit refinements or changes in the material models without difficulty. Further, the formulations retain a form that can be accommodated in conventional linear elastic procedures (e.g., the element stiffness matrix remains symmetrical, unlike some tangent stiffness formulations). Prestrain effects in the material components of an element can also be accommodated, enabling the consideration of such factors as prestressed reinforcement, concrete shrinkage, and thermal effects. Finally, the iterative calculations involved have demonstrated excellent stability and convergence characteristics.

Although specific formulations were presented for linear displacement elements only, the method can be used in developing higher order elements. Work is currently progressing in this direction.

Acknowledgments

The work presented in this paper was possible through funding from the

Natural Sciences and Engineering Research Council of Canada. The writer wishes to express his sincere gratitude for the support received.

APPENDIX I. STIFFNESS MATRIX COEFFICIENTS

For the rectangular linear displacement element shown in Fig. 4(*a*), the stiffness matrix coefficients corresponding to $\{r\} = [u_1\ u_2\ u_3\ u_4\ v_1\ v_2\ v_3\ v_4]$ are

$$k_{11} = k_{33} = 4b^2t_0D_{11} + 6abt_0D_{13} + 4a^2t_0D_{33}$$

$$k_{12} = k_{34} = -4b^2t_0D_{11} + 2a^2t_0D_{33}$$

$$k_{13} = -2b^2t_0D_{11} - 6abt_0D_{13} - 2a^2t_0D_{33}$$

$$k_{14} = k_{23} = 2b^2t_0D_{11} - 4a^2t_0D_{33}$$

$$k_{15} = k_{37} = 3abt_0D_{12} + 4b^2t_0D_{13} + 4a^2t_0D_{23} + 3abt_0D_{33}$$

$$k_{16} = k_{38} = 3abt_0D_{12} - 4b^2t_0D_{13} + 2a^2t_0D_{23} - 3abt_0D_{33}$$

$$k_{17} = k_{35} = -3abt_0D_{12} - 2b^2t_0D_{13} - 2a^2t_0D_{23} - 3abt_0D_{33}$$

$$k_{18} = k_{36} = -3abt_0D_{12} + 2b^2t_0D_{13} - 4a^2t_0D_{23} + 3abt_0D_{33}$$

$$k_{22} = k_{44} = 4b^2t_0D_{11} - 6abt_0D_{13} + 4a^2t_0D_{33}$$

$$k_{24} = -2b^2t_0D_{11} + 6abt_0D_{13} - 2a^2t_0D_{33}$$

$$k_{25} = k_{47} = -3abt_0D_{12} - 4b^2t_0D_{13} + 2a^2t_0D_{23} + 3abt_0D_{33}$$

$$k_{26} = k_{48} = -3abt_0D_{12} + 4b^2t_0D_{13} + 4a^2t_0D_{23} - 3abt_0D_{33}$$

$$k_{27} = k_{45} = 3abt_0D_{12} + 2b^2t_0D_{13} - 4a^2t_0D_{23} - 3abt_0D_{33}$$

$$k_{28} = k_{46} = 3abt_0D_{12} - 2b^2t_0D_{13} - 2a^2t_0D_{23} + 3abt_0D_{33}$$

$$k_{55} = k_{77} = 4a^2t_0D_{22} + 6abt_0D_{23} + 4b^2t_0D_{33}$$

$$k_{56} = k_{78} = 2a^2t_0D_{22} - 4b^2t_0D_{33}$$

$$k_{57} = -2a^2t_0D_{22} - 6abt_0D_{23} - 2b^2t_0D_{33}$$

$$k_{58} = k_{67} = -4a^2t_0D_{22} + 2b^2t_0D_{33}$$

$$k_{66} = k_{88} = 4a^2t_0D_{22} - 6abt_0D_{23} + 4b^2t_0D_{33}$$

$$k_{68} = -2a^2t_0D_{22} + 6abt_0D_{23} - 2b^2t_0D_{33}$$

$$k_{ij} = k_{ji};\quad t_0 = \frac{t}{(12ab)}$$

For the triangular linear displacement element shown in Fig. 4(*b*), the stiffness matrix coefficients corresponding to $\{r\} = [u_1\ u_2\ u_3\ v_1\ v_2\ v_3]$ are

$$k_{11} = b_1^2t_0D_{11} + 2a_1b_1t_0D_{13} + a_1^2t_0D_{33}$$

$$k_{12} = b_1b_2t_0D_{11} + (a_1b_2 + a_2b_1)t_0D_{13} + a_1a_2t_0D_{33}$$

$$k_{13} = b_1b_3t_0D_{11} + (a_1b_3 + a_3b_1)t_0D_{13} + a_1a_3t_0D_{33}$$

$$k_{14} = a_1b_1t_0D_{12} + b_1^2t_0D_{13} + a_1^2t_0D_{23} + a_1b_1t_0D_{33}$$

$$k_{15} = a_2b_1t_0D_{12} + b_1b_2t_0D_{13} + a_1a_2t_0D_{23} + a_1b_2t_0D_{33}$$

$$k_{16} = a_3b_1t_0D_{12} + b_1b_3t_0D_{13} + a_1a_3t_0D_{23} + b_1b_3t_0D_{33}$$

$$k_{22} = b_2^2t_0D_{11} + 2a_2b_2t_0D_{13} + a_2^2t_0D_{33}$$

$$k_{23} = b_2b_3t_0D_{11} + (a_2b_3 + a_3b_2)t_0D_{13} + a_2a_3t_0D_{33}$$

$$k_{24} = a_1b_2t_0D_{12} + b_1b_2t_0D_{13} + a_1a_2t_0D_{23} + a_2b_1t_0D_{33}$$

$$k_{25} = a_2b_2t_0D_{12} + b_2^2t_0D_{13} + a_2^2t_0D_{23} + a_2b_2t_0D_{33}$$

$$k_{26} = a_3b_2t_0D_{12} + b_2b_3t_0D_{13} + a_2a_3t_0D_{23} + a_2b_3t_0D_{33}$$

$$k_{33} = b_3^2t_0D_{11} + 2a_3b_3t_0D_{13} + a_3^2t_0D_{33}$$

$$k_{34} = a_1b_3t_0D_{12} + b_1b_3t_0D_{13} + a_1a_3t_0D_{23} + a_3b_1t_0D_{33}$$

$$k_{35} = a_2b_3t_0D_{12} + b_2b_3t_0D_{13} + a_2a_3t_0D_{23} + a_3b_2t_0D_{33}$$

$$k_{36} = a_3b_3t_0D_{12} + b_3^2t_0D_{13} + a_3^2t_0D_{23} + a_3b_3t_0D_{33}$$

$$k_{44} = a_1^2t_0D_{22} + 2a_1b_1t_0D_{23} + b_1^2t_0D_{33}$$

$$k_{45} = a_1a_2t_0D_{22} + (a_1b_2 + a_2b_1)t_0D_{23} + b_1b_2t_0D_{33}$$

$$k_{46} = a_1a_3t_0D_{22} + (a_1b_3 + a_3b_1)t_0D_{23} + b_1b_3t_0D_{33}$$

$$k_{55} = a_2^2t_0D_{22} + 2a_2b_2t_0D_{23} + b_2^2t_0D_{33}$$

$$k_{56} = a_2a_3t_0D_{22} + (a_2b_3 + a_3b_2)t_0D_{23} + b_2b_3t_0D_{33}$$

$$k_{66} = a_3^2t_0D_{22} + 2a_3b_3t_0D_{23} + b_3^2t_0D_{33}$$

$$k_{ij} = k_{ji}; \quad t_0 = \frac{1}{2}\,t\left(\frac{a_2b_1 - a_1b_2}{a_2b_3 - a_3b_2}\right)^2$$

$$a_1 = x_3 - x_2 \qquad a_2 = x_1 - x_3 \qquad a_3 = x_2 - x_1$$

$$b_1 = y_2 - y_3 \qquad b_2 = y_3 - y_1 \qquad b_3 = y_1 - y_2$$

APPENDIX II. SAMPLE CALCULATIONS

Step 0

Given

$f'_c = 21.8$ MPa $\quad f_{cr} = 1.54$ MPa $\quad E_c = 24{,}200$ MPa
$\epsilon_0 = -0.0018 \quad \nu = 0.30 \quad E_s = 200{,}000$ MPa
$\rho_x = 0.02195 \quad \rho_y = 0 \quad f_{yx} = 402$ MPa
$a = 890$ mm $\quad b = 890$ mm $\quad t = 70$ mm

Step 1

Given $f_x = 3.10$ MPa, $f_y = 0$, $v_{xy} = 1.0$ MPa

$[F] = [H_2 \; H_3 \; H_4 \; V_3 \; V_4]$

$= [65.41 \;\; 127.71 \;\; -65.41 \;\; 31.15 \;\; -31.15]$ (kN)

Step 2

No prestrains, $[\epsilon_c^o] = [\epsilon_s^o]_1 = [0 \;\; 0 \;\; 0]$

Step 3

Given (from previous iteration)

$[\epsilon] = [0.669 \;\; 0.560 \;\; 1.310] \times 10^{-3}$

a. Determine principal strain conditions (using general strain compatibility).

$\epsilon_{c1} = 1.272 \times 10^{-3} \qquad \epsilon_{c2} = -0.0427 \times 10^{-3}$
$\theta_c = 47.38° \qquad \epsilon_{s1} = 0.669 \times 10^{-3}$

b. Determine principal stresses in concrete/reinforcement

from Eq. 21 $f_{c1} = 1.024$ MPa
from Eq. 15 $f_{c2} = -0.925$ MPa
from Eq. 22 $f_{s1} = 133.9$ MPa

c. Evaluate secant moduli

from Eq. 4 $\bar{E}_{c1} = f_{c1}/\epsilon_{c1} = 805$ MPa
from Eq. 5 $\bar{E}_{c2} = f_{c2}/\epsilon_{c2} = 21{,}650$ MPa
from Eq. 6 $\bar{G}_c = \bar{E}_{c1}\bar{E}_{c2}/(\bar{E}_{c1} + \bar{E}_{c2}) = 776$ MPa
from Eq. 8 $\bar{E}_{s1} = f_{s1}/\epsilon_{s1} = 200{,}000$ MPa

Step 4

a. Determine concrete material stiffness matrix, $[D_c]$:

from Eq. 3 $$[D_c]' = \begin{bmatrix} 21{,}650 & 0 & 0 \\ 0 & 805 & 0 \\ 0 & 0 & 776 \end{bmatrix} \text{(MPa)}$$

from Eq. 13 $\psi = 132.62°$

from Eq. 12 $$[T_c] = \begin{bmatrix} 0.4585 & 0.5415 & -0.4983 \\ 0.5415 & 0.4585 & 0.4983 \\ 0.9966 & -0.9966 & -0.0830 \end{bmatrix}$$

from Eq. 10 $$[D_c] = [T_c]^T[D_c]'[T_c] = \begin{bmatrix} 5{,}558 & 4{,}805 & -4{,}794 \\ 4{,}805 & 7{,}287 & -5{,}593 \\ -4{,}794 & -5{,}593 & 5{,}580 \end{bmatrix} \text{(MPa)}$$

b. Determine reinforcement material stiffness matrices, $[D_s]_i'$; $1 < i < n$, $n = 1$:

from Eq. 7 $$[D_s]_1' = \begin{bmatrix} 4{,}390 & 0 & 0 \\ 0 & 0 & 0 \\ 0 & 0 & 0 \end{bmatrix} \text{(MPa)}$$

from Eq. 14 $\psi = 0°$

from Eq. 12 $$[T_s]_1 = \begin{bmatrix} 1 & 0 & 0 \\ 0 & 1 & 0 \\ 0 & 0 & 1 \end{bmatrix}$$

from Eq. 11 $$[D_s]_1 = [T_s]_1^T[D_s]_1'[T_s]_1 = \begin{bmatrix} 4{,}390 & 0 & 0 \\ 0 & 0 & 0 \\ 0 & 0 & 0 \end{bmatrix} \text{(MPa)}$$

Step 5

Determine composite material stiffness matrix $[D]$ from Eq. 9:

$$[D] = [D_c] + \sum_{i=1}^{n} [D_s]_i$$

$$= \begin{bmatrix} 9{,}948 & 4{,}805 & -4{,}794 \\ 4{,}805 & 7{,}287 & -5{,}593 \\ -4{,}794 & -5{,}593 & 5{,}580 \end{bmatrix} \text{(MPa)} = \begin{bmatrix} D_{11} & D_{12} & D_{13} \\ D_{21} & D_{22} & D_{23} \\ D_{31} & D_{32} & D_{33} \end{bmatrix}$$

Step 6

Formulate element stiffness matrix (using coefficients in Appendix III):

$$[k] = \begin{bmatrix} 194.6 & -167.0 & -13.4 & -14.1 & -60.6 & 33.0 & -60.6 & 88.2 \\ & 530.1 & -14.1 & -348.9 & 60.2 & -424.1 & 61.0 & 302.9 \\ & & 194.6 & -167.0 & -60.6 & 88.2 & -60.6 & 33.0 \\ & & & 530.1 & 61.0 & 302.9 & 60.2 & -424.1 \\ & & & & 104.5 & -45.2 & 45.6 & -104.9 \\ & \text{symmetric} & & & & 496.0 & -104.9 & -345.9 \\ & & & & & & 104.5 & -45.2 \\ & & & & & & & 496.0 \end{bmatrix} \text{(kN/mm)}$$

Step 7

Determine element prestrain displacements:

No prestrains, $[r_c^o] = [r_s^o] = [0]$

Step 8

Determine prestrain joint loads:

no prestrains, $[F^*] = 0$

Step 9

Determine nodal force vector, $[F']$:

$[F'] = [F] + [F^*] = [65.41 \quad 127.71 \quad -65.41 \quad 31.15 \quad -31.15]$ (kN)

Step 10

Assemble structure stiffness matrix, eliminating freedoms corresponding to fixed joints (i.e., u_1, v_1, v_2):

$$[K] = \begin{bmatrix} 530.1 & -14.1 & -348.9 & 61.0 & 302.9 \\ & 194.6 & -167.0 & -60.6 & 33.0 \\ & & 530.1 & 60.2 & -424.1 \\ & \text{symmetric} & & 104.5 & -45.2 \\ & & & & 496.0 \end{bmatrix} \text{(kN/mm)}$$

Step 11

Invert stiffness matrix:

$$[K]^{-1} = \begin{bmatrix} 8.449 & 9.397 & 12.945 & -4.842 & 4.842 \\ & 26.804 & 27.091 & 1.278 & 15.757 \\ & & 35.828 & -3.564 & 20.599 \\ & & & 15.738 & 1.259 \\ & \text{symmetric} & & & 15.738 \end{bmatrix} \times 10^{-3} \text{ (mm/kN)}$$

Step 12

Compute joint displacements:

$\{r\} = [K]^{-1}[F']$

$$= \begin{bmatrix} 8.449 & 9.397 & 12.945 & -4.842 & 4.842 \\ & 26.804 & 27.091 & 1.278 & 15.757 \\ & & 35.828 & -3.564 & 20.599 \\ & & & 15.738 & 1.259 \\ & & & & 15.738 \end{bmatrix} \begin{bmatrix} 65.41 \\ 127.71 \\ -65.41 \\ 31.15 \\ -31.15 \end{bmatrix} \times 10^{-3} = \begin{bmatrix} 0.604 \\ 1.815 \\ 1.210 \\ 0.531 \\ 0.531 \end{bmatrix} \text{ (mm)}$$

thus $u_1 = 0$ $u_2 = 0.604$ mm $u_3 = 1.815$ mm $u_4 = 1.210$ mm
$v_1 = 0$ $v_2 = 0$ $v_3 = 0.531$ mm $v_4 = 0.531$ mm

Step 13

Determine element strains:

$$\epsilon_x = \frac{u_2 + u_3 - u_1 - u_4}{2a} = 0.679 \times 10^3$$

$$\epsilon_y = \frac{v_3 + v_4 - v_1 - v_2}{2b} = 0.596 \times 10^{-3}$$

$$\gamma_{xy} = \frac{u_3 + u_4 - u_1 - u_2}{2b} + \frac{v_2 + v_3 - v_1 - v_4}{2a} = 1.360 \times 10^{-3}$$

Note strains changed from starting values in Step 1.

Step 14

Check element stresses:

$$\{f\} = [D_c](\{\epsilon\} - \{\epsilon_c^o\}) + \Sigma[D_s]_i(\{\epsilon\} - \{\epsilon_s^o\}_i)$$

$$= \begin{bmatrix} 9{,}948 & 4{,}805 & -4{,}794 \\ 4{,}805 & 7{,}287 & -5{,}593 \\ -4{,}794 & -5{,}593 & 5{,}580 \end{bmatrix} \begin{bmatrix} 0.000679 \\ 0.000596 \\ 0.001360 \end{bmatrix} = \begin{bmatrix} 3.10 \\ 0 \\ 1.00 \end{bmatrix} \text{ (MPa)}$$

Agreement with imposed load condition.

Step 15

Recompute secant moduli (as per Step 3):

$\bar{E}'_{c1} = 771$ MPa $\quad \bar{E}'_{c2} = 21{,}558$ MPa

$\bar{G}'_c = 745$ MPa $\quad \bar{E}'_{s1} = 200{,}000$ MPa

Step 16

Moduli not converged, go to Step 4.

APPENDIX III. REFERENCES

Balakrishnam, S., and Murray, D. W. (1988). "Concrete constitutive model for NLFE analysis of structures." *J. Struct. Engrg.*, ASCE, 114(7), 1449–1466.

Ang, B. G. (1985). "Seismic shear strength of circular bridge piers." Thesis presented to the University of Canterbury, at Christchurch, New Zealand, in partial fulfillment of the requirements for the degree of Doctor of Philosophy.

Barzegar-Jamshidi, F., and Schnobrich, W. C. (1986). "Nonlinear finite element analysis of reinforced concrete under short term monotonic loading." *Civil Engrg. Studies Report No. 530,* Univ. of Illinois at Urbana-Champaign.

Bhide, S. B., and Collins, M. P. (1987). "Reinforced concrete elements in shear and tension." *Publication No. 87-02,* Dept. of Civil Engineering, Univ. of Toronto, Toronto, Ontario, Canada.

Cervenka, V. (1970). "Inelastic finite element analysis of reinforced concrete panels." Thesis presented to the University of Colorado, at Boulder, Colo., in partial fulfillment of the requirements for the degree of Doctor of Philosophy.

Mau, S. T., and Hsu, T. T. C. (1987). "Shear behaviour of reinforced concrete framed wall panels with vertical loads." *Amer. Concrete Inst. Struct. J.*, 84(3), 228–234.

Meyboom, J. (1987). "An experimental investigation of partially prestressed, orthogonally reinforced concrete elements subjected to membrane shear." Thesis presented to the University of Toronto, Toronto, Ontario, Canada, in partial fulfillment of the requirements for the degree of Master of Applied Science.

Niwa, J., Maekawa, K., and Okamura, H. (1981). "Nonlinear finite element analysis of deep beams." *Int. Assoc. for Bridge and Struct. Engrg. Colloquium, Final Report, Delft,* The Netherlands, 335–350.

Stevens, N. J., et al. (1987). "Analytical modelling of reinforced concrete subjected to monotonic and reversed loadings." *Publication No. 87-1,* Dept. of Civ. Engineering, Univ. of Toronto, Toronto, Ontario, Canada.

Vecchio, F. J., and Collins, M. P. (1986). "The modified compression field theory for reinforced concrete elements subjected to shear." *J. Amer. Concrete Inst.*, 83(2), 219–231.

Vecchio, F. J. (1989). "Nonlinear finite element analysis of reinforced concrete membranes." *Amer. Concrete Inst. Struct. J.*, 86(1), 26–35.
Yang, T. Y. (1986). *Finite element structural analysis*, Prentice-Hall, New Jersey.

APPENDIX IV. NOTATION

The following symbols are used in this paper:

$[B]$ = element strain function matrix;
$[D]$ = composite material stiffness matrix;
$[D_c]$ = concrete material stiffness matrix;
$[D_s]$ = reinforcement material stiffness matrix;
E = modulus of elasticity of linear isotropic material;
E_c = modulus of elasticity of concrete (initial tangent stiffness);
$\bar{E}_{c1}$ = secant modulus of concrete in principal tensile strain direction;
$\bar{E}_{c2}$ = secant modulus of concrete in principal compressive strain direction;
$\bar{E}_{si}$ = secant modulus of reinforcement in i direction;
$[F]$ = structure nodal force matrix, applied forces;
$[F^*]$ = structure nodal force matrix, prestrain forces;
$[F']$ = structure nodal force matrix, total forces;
$\{f\}$ = element stress matrix;
f'_c = compressive strength of concrete cylinder;
f_{c1} = average principal tensile stress in concrete;
f_{c2} = average principal compressive stress in concrete;
f_{cr} = concrete cracking stress;
f_{si} = average stress in i direction reinforcement;
f_x = element stress in x direction;
f_y = element stress in y direction;
f_{yi} = yield stress of i direction reinforcement;
$\bar{G}_c$ = secant shear modulus of concrete;
$[K]$ = structure stiffness matrix;
$[k]$ = element stiffness matrix;
$\{r\}$ = structure nodal displacement matrix;
$[T]$ = transformation matrix;
v_{xy} = shear stress on element, relative to x, y axes;
α = orientation of reinforcement relative to element x, y axes;
β = orientation of element x, y axes relative to global X, Y axes;
$\{\epsilon\}$ = element strain matrix;
ϵ_c^o = initial free strain in concrete;
ϵ_{c1} = average principal tensile strain in concrete;
ϵ_{c2} = average principal compressive strain in concrete;
ϵ_{cr} = strain in concrete at cracking;
ϵ_0 = strain in concrete cylinder at peak stress f'_c (negative quantity);
ϵ_s^o = initial free strain in reinforcement;
ϵ_{si} = strain in i direction reinforcement;
ϵ_x = strain in x direction;
ϵ_y = strain in y direction;
γ_{xy} = shear strain relative to x, y axes;
θ_c = angle of inclination of principal stresses/strains in concrete;
ρ_i = steel reinforcement ratio in i-direction;
ϕ = orientation of crack direction relative to element x, y axes; and
ψ = rotation angle in transformation matrix.